INTERACTION DIAGRAMS FOR FRP STRENGTHENED RC RECTANGULAR COLUMNS WITH LARGE ASPECT RATIO

Sreelatha Vuggumudi [a,*], P. Alagusundaramoorthy[b]

[a]Doctoral student, Structural Engineering Laboratory, IIT Madras, India 600036.

[b]Professor, Structural Engineering Laboratory, IIT Madras, India 600036.

[*]Corresponding Author

Sreelatha Vuggumudi

Doctoral Student, Structural Engineering Laboratory

Civil Engineering Department, IIT Madras

Chennai 600036

Tamilnadu

India

Mob: +91- 94947 50640

E-mail: srilathavuggumudi.91@gmail.com

Abstract

The load carrying capacity of reinforced concrete columns (RC) shall be enhanced by providing lateral confinement using fiber reinforced polymer (FRP). As per ACI 440.2R-08 [1], external strengthening using FRP composites is more effective for circular columns than rectangular columns having an aspect ratio greater than 2.0. The main objective is to develop column interaction diagrams for RC rectangular columns having an aspect ratio greater than 2.0 externally strengthened using FRP composites without any shape modification and subjected to combined axial load (P_n) and bending moment (M_n) due to lateral loading. Tests are conducted and semi-empirical equations developed for FRP strengthened RC rectangular columns with large aspect ratio. P_n - M_n interactions diagrams are developed using the semi-empirical solutions and validated with 3D finite element analysis. The column interaction diagrams are developed by varying the unconfined compressive strength of concrete, yield strength of steel, percentage of steel reinforcement and thickness of FRP composite. These diagrams shall be used for the design of FRP strengthened RC rectangular columns with large aspect ratio.

Key words: P_n - M_n interaction diagrams; Semi-empirical solutions; Finite element analysis; RC rectangular columns; FRP composites; Large aspect ratio; shape modification.

1. Introduction

The performance of a building is defined by its structural stability, life safety and operation. The majority of existing buildings and bridges were designed using the old codal provisions. In accordance to the revised standards, certain structures are not satisfying the requirement and need to be strengthened. Columns being the primary load bearing members in structures, might require to be strengthened to increase the flexural and shear strength, deformation capacity, rotation at the beam-column junction and strengthen the regions of non-standard splicing of longitudinal bars. External strengthening using FRP composite is more effective than steel and concrete jacketing due to its high strength to weight ratio, high stiffness to weight ratio and excellent corrosion resistance. Due to the uniform distribution of lateral confining pressure in circular sections, circular columns can be effectively strengthened using FRP composites compared to square and rectangular columns. The confining pressure is maximum at the corners and varying non-uniformly in between the corners in square and rectangular sections.

Extensive research work has been reported on axially loaded RC circular columns and rectangular columns having aspect ratio less than 2.0 externally strengthened with FRP composites. Parvin and Jamwal [6] studied influence of wrap thickness, wrap ply angle configuration and concrete strength on the axial capacity of columns through nonlinear finite element analysis. Pedro et al. [7] studied the effect of shape of cross section and corner radii on the strength of column under axial compression. Chen and Togay [4] and Mohammad et al. [10] tested square and rectangular FRP tubes filled with concrete under axial loading. Alsayed et al. [2], Prota et al. [8], Tan [13] and Tanwongsval et al. [14] predicted the confinement effect of FRP composites on small scale wall-like RC columns with rectangular and elliptical cross sections having high aspect ratio 3.65 under axial and sustained axial loading. Lam and Teng [5] and Teng and Lam [15, 16] developed a stress-strain model based on the experiments and existing studies to predict the behavior of FRP confined square and elliptical RC columns under axial loading. Challal et. al. [3] and Mimiran and Shahawy [9] developed analytical models to predict the axial load carrying capacity of small scale FRP confined RC columns. Seible et al. [11] and Wang and Hsu [17] proposed a design method to evaluate the load carrying capacity of square and rectangular RC columns with aspect ratio less than 2.0 confined with FRP composites under axial and combined axial and lateral loading with shape modification. As can be observed, test data, semi-empirical solutions, finite element models and P_n - M_n interactions diagrams are not available for FRP strengthened RC rectangular columns having aspect ratio greater than 2.0 without any modification of cross section and subjected to combined axial and lateral loading.

2. Objective and Scope

The main objective of the study is to develop P_n - M_n interaction diagrams for RC rectangular columns having an aspect ratio greater than 2.0 externally strengthened using FRP composites without any shape modification and subjected to combined axial and lateral loading.

The scope of work is limited to (i) developing finite element (FE) models for FRP strengthened RC rectangular columns and validating with the test data and (ii) comparing the proposed semi-empirical solutions with FE models and (iii) developing P_n - M_n interaction diagrams using semi-empirical solutions and FE models by varying the unconfined compressive strength of concrete, yield strength of steel, percentage of steel reinforcement and thickness of FRP composite.

3. Experimental Study

Six prototype RC rectangular columns of length (l) 3000 mm, breadth (b) 600 mm and depth (D) 230 mm designated as CCA1 (control column under axial load), RCA2 (retrofitted column under axial load), CCL3, RCL4, CCC5 and RCC6 were cast. The strengthening scheme and loading pattern of tested columns are given in Table 1. The column RCC6 was clamped at one end and the other end kept free. An axial compressive load up to 600 kN was applied at the free end and maintained constant. An incremental lateral load was also applied at the free end in such a way that the column was subjected to weak axis bending. Based on the strain measurements, it is noted that the failure of column RCC6 was initiated by cracking of CFRP composite perpendicular to the longitudinal axis of the column and followed by yielding of steel reinforcement. No major cracks were observed in the column.

Table 1 Details of Tested Specimens

Specimen	Strengthening scheme	Loading pattern
CCA1	-	Axial load
RCA2	Two layers of carbon fibre fabric of uni-directional cloth (UDC) 430 gsm (t_{frp} = 1.2mm)	Axial load
CCL3	-	Lateral load (weak axis bending)
RCL4	Two layers of carbon fibre fabric of UDC 430 gsm (t_{frp} = 1.2mm)	Lateral load (weak axis bending)
CCC5		Combined loading
RCC6	Two layers of carbon fibre fabric of UDC 430 gsm (t_{frp} = 1.2mm)	Combined loading

The axial and lateral load carrying capacity of tested columns is calculated using the semi-empirical solutions available in the literature for columns with aspect ratio less than 2.0 without partial safety factors and compared with the test data. It is observed that the semi-empirical solutions are under estimating and over estimating the axial and lateral load carrying capacity of FRP strengthened RC rectangular columns with aspect ratio greater than 2.0 up to 22% and 17% respectively.

4. Semi-Empirical Solutions

The procedure given in ACI 440.2R-08 is modified for FRP strengthened RC rectangular columns having aspect ratio greater than 2.0 without shape modification of cross section. New semi-empirical solutions are proposed to calculate the load carrying capacity of these columns subjected to axial, lateral and combined axial and lateral loading.

The axial capacity of FRP strengthened RC columns without any partial safety factors is calculated using Eqn. (1).

$$P_n = [f'_{co} + k_1 k_a f_l](A_g - A_{st}) + f_y A_{st} \quad (1)$$

In which, f'_{co} is the unconfined compressive strength of concrete, f_y is the yield strength of steel, $A_g$is the gross sectional area of column, A_{st} is the area of steel reinforcement, f_l is the lateral confining pressure and k_1 and k_a are the shape factors. The value of 'k_1' obtained is 1.78 from test data by trial and error method. k_a can be calculated using the equations given in Sreelatha and Alagusundaramoorthy [12].

The representative P_n - M_n interaction diagram is shown in Fig. 1. Point 'A' represents the column under pure axial compression, point 'B' corresponds to ultimate compressive strain (ε'_{ccu}) at the extreme compression fiber and zero strain at the extreme layer of tensile reinforcement, point 'C' corresponds to ultimate compressive strain at the extreme compression fiber (ε'_{ccu}) and yielding tensile strain (ε_{sy}) at the extreme layer of tensile reinforcement and point 'D' represents pure bending.

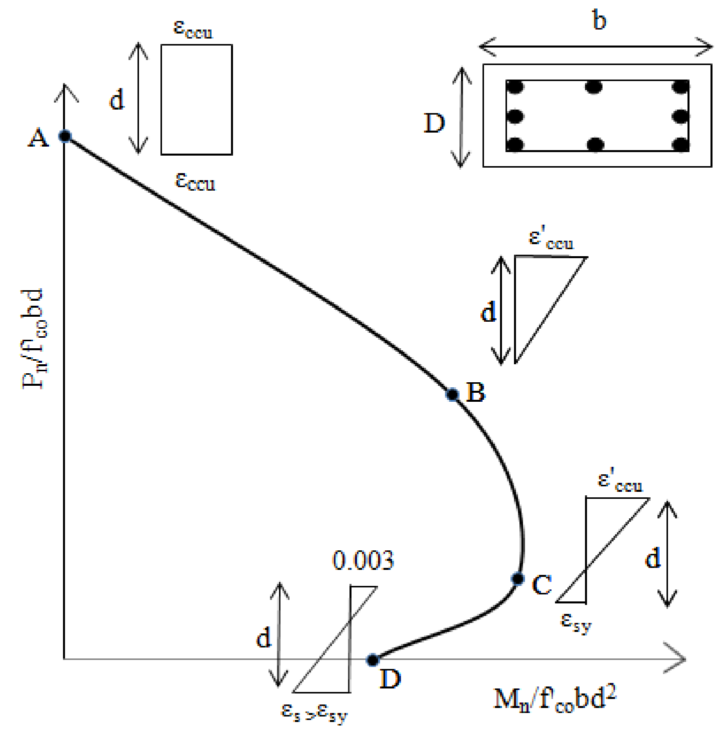

Fig. 1. Representative Interaction Diagram

The P_n - M_n co-ordinates at point B and C (Fig. 1) are calculated using Eqns. (2) and (3).

$$P_{n(B,C)} = [A(y_t)^3 + B(y_t)^2 + C(y_t) + D] + \sum A_{si} f_{si} \tag{2}$$

$$M_{n(B,C)} = [E(y_t)^4 + F(y_t)^3 + G(y_t)^2 + H(y_t) + kI] + \sum A_{si} f_{si} d_i \quad (3)$$

The parameters A, B, C, D, E, F, G, H, I, y_t, A_{si}, f_{si} and d_i are calculated as per the equations given in ACI 440.2R-08. Values of constant 'k' are obtained from the test data as 1.12 and 1.55 for lateral load and combined axial and lateral loading respectively by trial and error method. The semi-empirical solutions are validated with the test data and the uncertainty parameters such as mean value, standard deviation and coefficient of variation (COV) are calculated as 1.000, 0.035 and 3.550 respectively.

5. Finite Element Analysis

Unstrengthened and strengthened 3D models of RC columns are generated using the finite element analysis (FEA) software ABAQUS. Solid C3D8R elements, Truss T3D2 elements and Shell S4R elements are used to model concrete, steel reinforcement and FRP composite. The steel reinforcement cage is embedded into concrete using EMBED constraint. FRP composite is modeled separately and connected to concrete substrate using TIE and SHELL SOLID COUPLING constraints. The shell-to-solid coupling is enforced by the automatic creation of an internal set of distributing coupling constraints between the nodes on the shell edge and nodes on the solid surface. An optimum mesh size of 100 mm is arrived from the convergence study. Static Riks analysis with arc length control is used for non linear analysis of RC columns.

The developed FE models for all columns is analyzed and compared with the test data and the explanation is provided for column RCC6. Fixed boundary condition is ensured at one end by arresting the translations U_X, U_Y and U_Z and rotations θ_X, θ_Y, θ_Z at and the other end is kept free. The specimen RCC6 is strengthened with 1.2 mm thick CFRP composite and S4R shell element is used to model 1.2 mm thick FRP composite. Axial load up to 600 kN is applied on the free end in one single load step using static general analysis and kept constant. An incremental lateral load is also applied on the free end in the second step using static Riks analysis till yield strain 4940 µm/m is reached in the longitudinal steel reinforcement and the analysis terminates automatically. The failure pattern of column RCC6 obtained from the finite element model closely predicts the experimental failure pattern (Fig. 2). The lateral load/lateral deflection is obtained from FEA and compared with the corresponding experimental curve (Fig. 3).

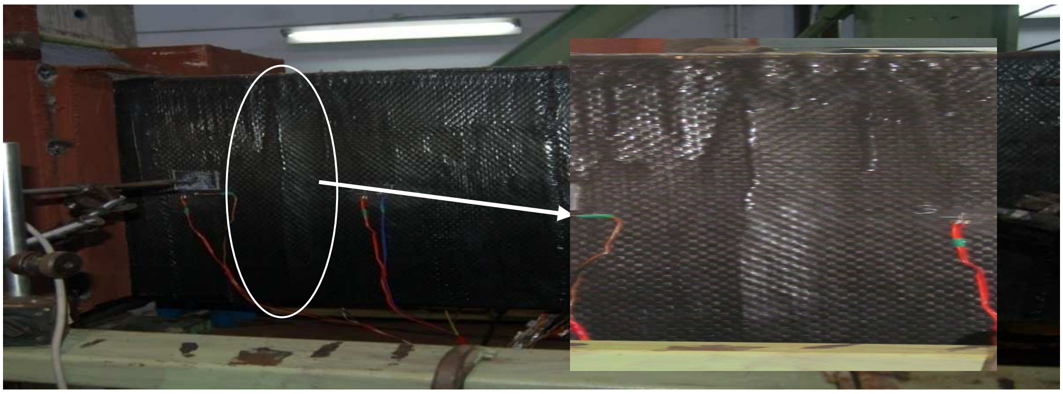

(a)

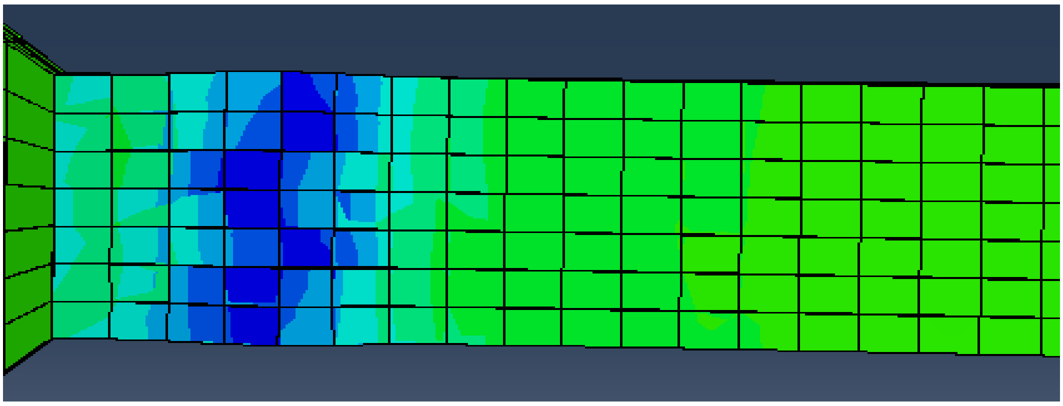

(b)

Fig. 2. Failure Pattern of Column RCC6 (a) Test (b) FEA

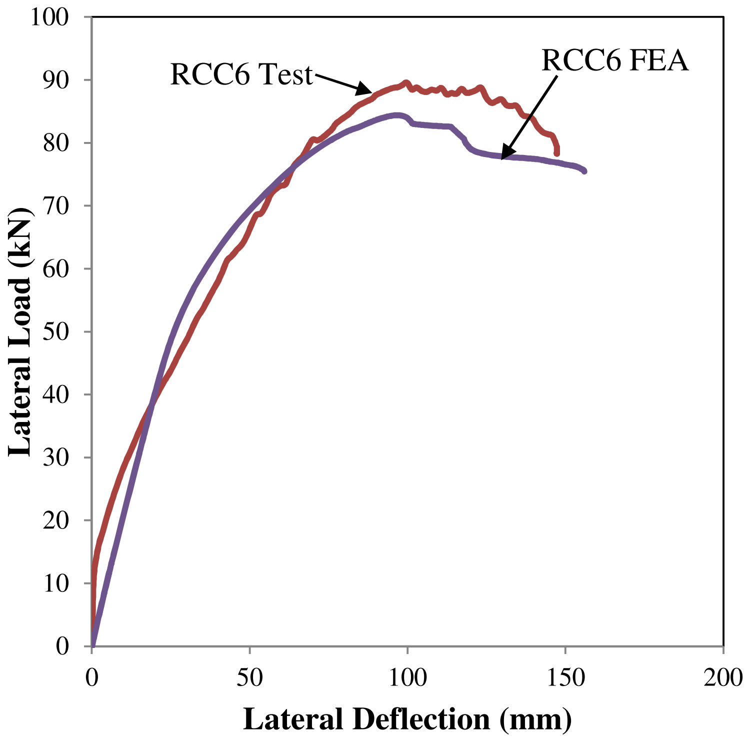

Fig. 3. Lateral Load/Lateral Deflection Curves of Column RCC6

FE models are developed for two standard FRP strengthened RC rectangular columns of cross section 600 mm (*b*) × 230 mm (*d*) to validate the P_n - M_n interaction diagrams. The first column modeled with concrete of strength 20 N/mm^2 reinforced with six 25 mm dia. steel rebars having yield strength 415 N/mm^2 distributed on two longer faces. The percentage of steel reinforcement (ρ_s) is 2.1. The column is strengthened with 1.8 mm thick CFRP composite which consist of three layers. The second column is developed for concrete of strength 30 N/mm^2 reinforced with eight 20 mm dia. steel rebars of yield strength 500 N/mm^2 distributed equally on four sides. The percentage of steel reinforcement (ρ_s) is 1.8. The column is strengthened with 1.2 mm thick CFRP composite which consist of two layers.

P_n - M_n interaction diagrams are generated from the salient points A, B, C and D (Fig. 3) obtained through FE models and compared with the corresponding curves developed by semi-empirical equations (Fig. 4). It is observed that the interaction diagrams developed by FEM validated well with the curves generated by semi-empirical solutions.

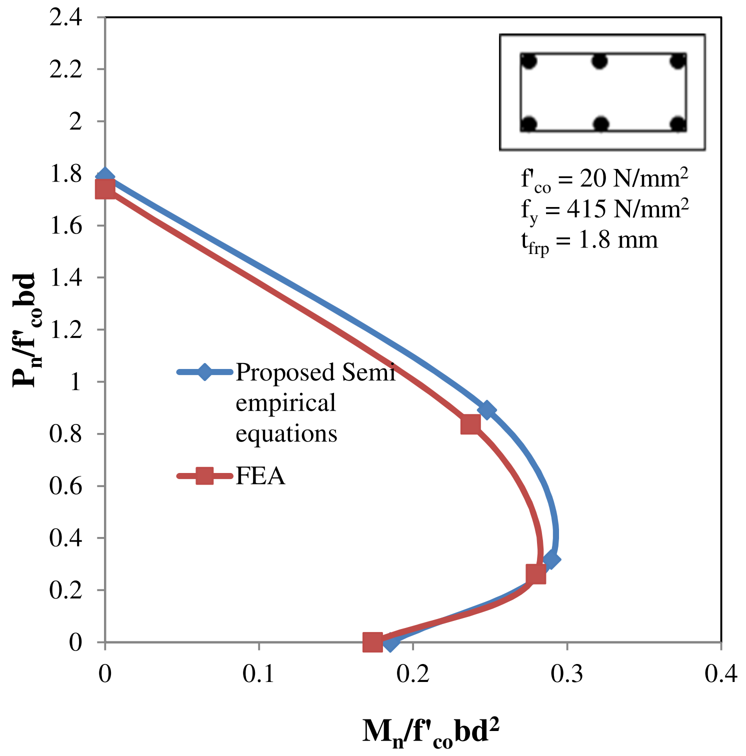

(a)

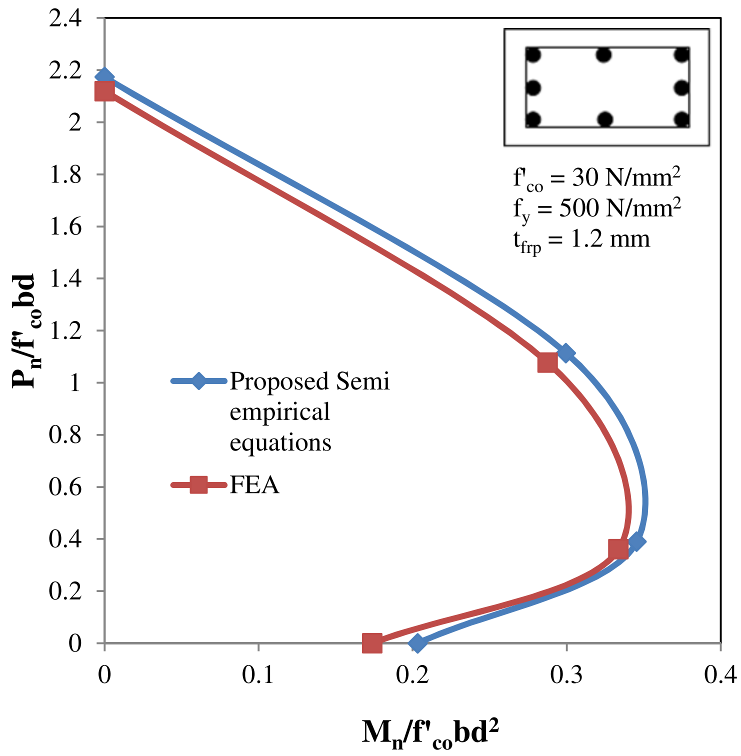

(b)

Fig. 4. Comparison of P_n - M_n interaction diagram

6. P_n - M_n Interaction Diagrams

P_n - M_n interaction diagrams are developed using the proposed semi-empirical solutions and 3D finite element models by varying the unconfined compressive strength of concrete (f'_{co}), yield strength of steel (f_y), percentage of steel reinforcement (ρ_s) and thickness of FRP composite (t_{frp}) for FRP strengthened RC columns with aspect ratio greater than 2.0 and without any shape modification. The values of $P_n/f'_{co}bd$ and $M_n/f'_{co}bd^2$ are obtained at four different points (Fig. 1).

Influence of f'_{co}, f_y and t_{frp} on lateral load carrying capacity of FRP strengthened RC rectangular column subjected to combined axial and lateral loading is studied for various percentage of steel reinforcement as 0.6 %, 1.1%, 1.8%, 2.1% and 2.6% and assuming that the steel reinforcement is distributed equally on two opposite sides. The value of f'_{co} considered in this study is 20 N/mm^2, 30 N/mm^2 and 40 N/mm^2. The yield strength of steel reinforcement considered is 415 N/mm^2 and 500 N/mm^2. The thickness of FRP composite is varied from 0.6 mm (1 layer of FRP composite), 1.2 mm (2 layers of FRP composite) and 1.8 mm (3 layers of FRP composite) and the P_n - M_n interaction diagrams for f'_{co} 20 N/mm^2 and f_y 415 N/mm^2 and 500 N/mm^2 are shown in Figs. 5 and 6. P_n - M_n interaction diagrams for FRP strengthened RC columns with f'_{co} 30 N/mm^2 and 40 N/mm^2 are shown in Figs. 7 to 10. From the interaction diagrams, it is observed that the lateral load carrying capacity is directly proportional to the unconfined compressive strength of concrete, yield strength of steel, thickness of FRP composite and percentage of steel reinforcement.

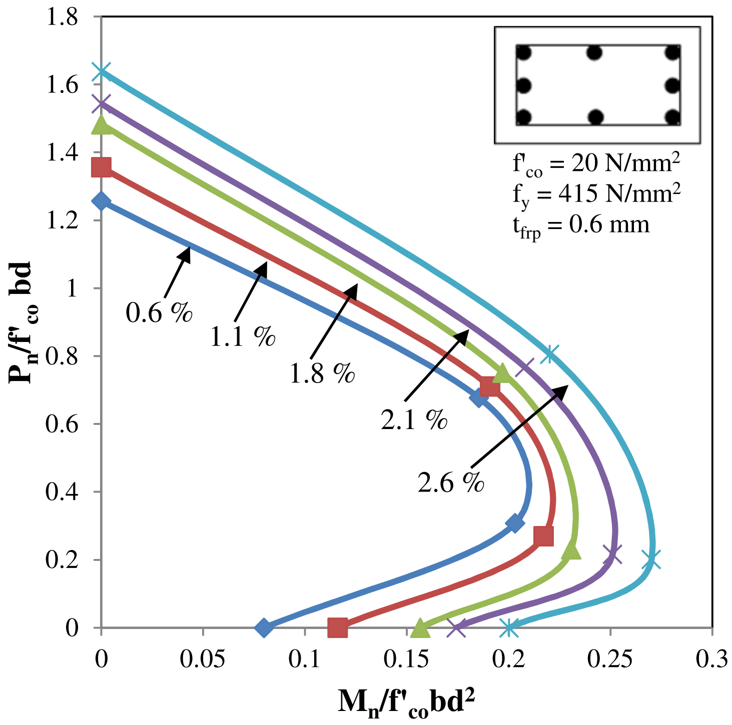

f'co = 20 N/mm2
fy = 415 N/mm2
tfrp = 0.6 mm
0.6 %
1.1 %
1.8 %
2.1 %
2.6 %
Pn/f'co bd
Mn/f'cobd2

(a)

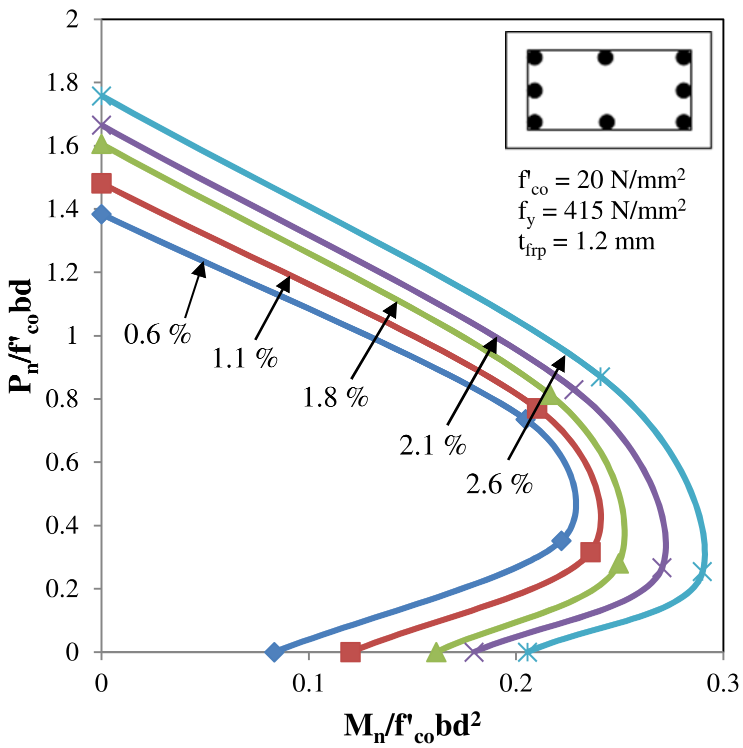

f'co = 20 N/mm2
fy = 415 N/mm2
tfrp = 1.2 mm
0.6 %
1.1 %
1.8 %
2.1 %
2.6 %
Pn/f'cobd
Mn/f'cobd2

(b)

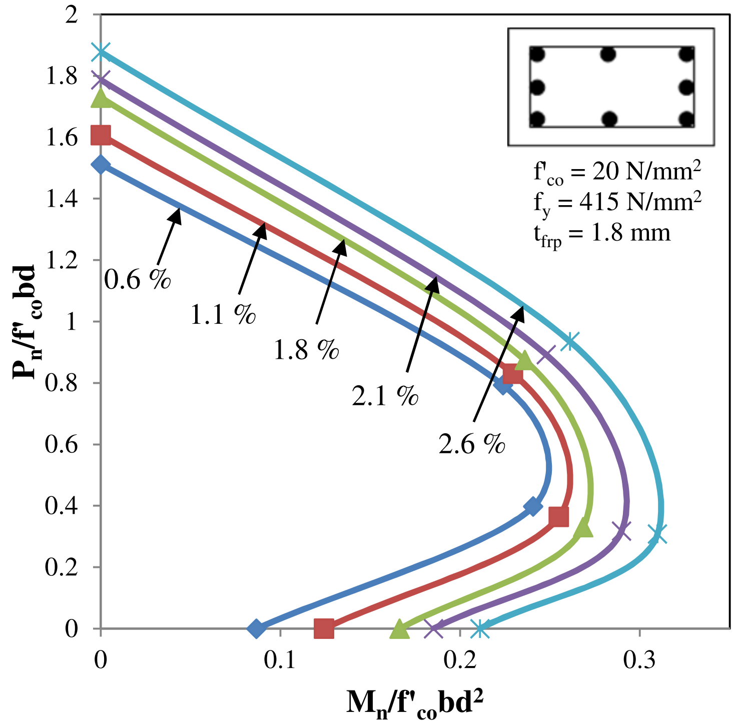

(c)

Fig. 5. P_n - M_n interaction diagrams for f'_{co} 20 N/mm^2 and f_y 415 N/mm^2 (a) t_{frp} 0.6 mm, (b) t_{frp} 1.2 mm and (c) t_{frp} 1.8 mm

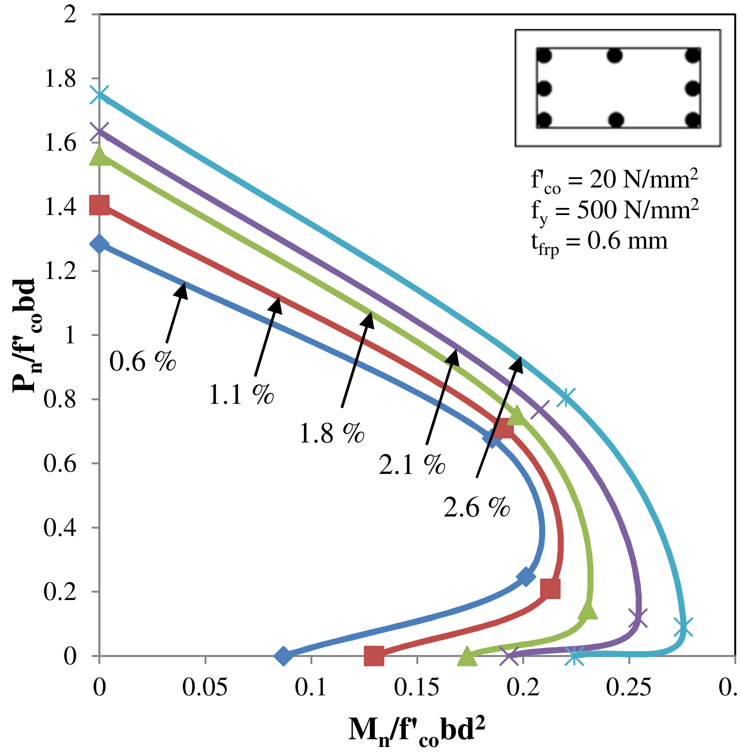

(a)

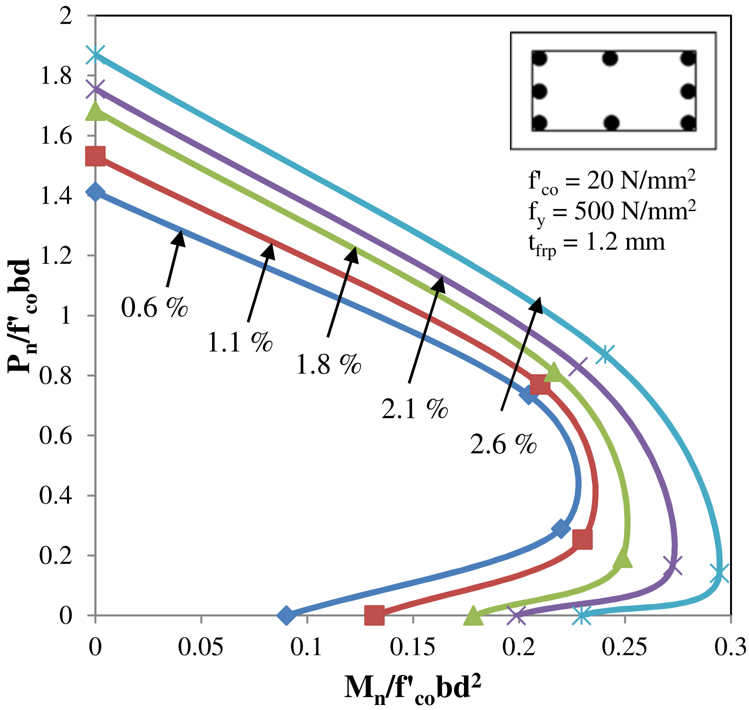

(b)

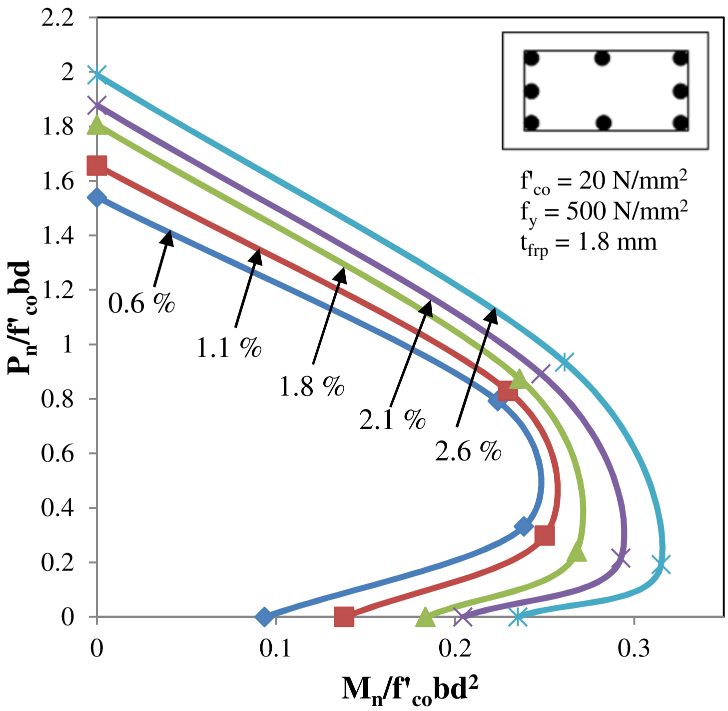

(c)

Fig. 6. P_n - M_n interaction diagrams for f'_{co} 20 N/mm^2 and f_y 500 N/mm^2 (a) t_{frp} 0.6 mm, (b) t_{frp} 1.2 mm and (c) t_{frp} 1.8 mm

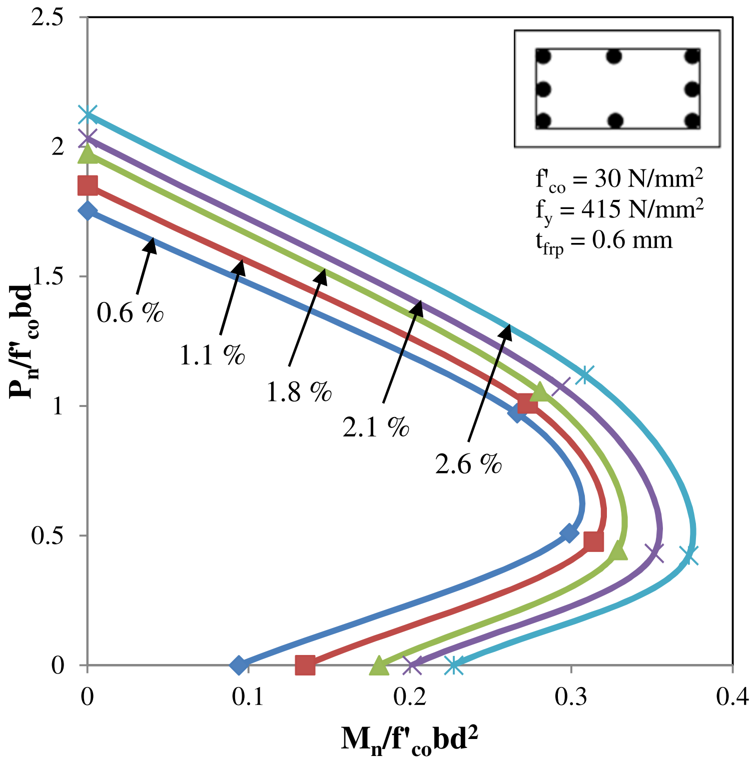
f'co = 30 N/mm2
fy = 415 N/mm2
tfrp = 0.6 mm
0.6 %
1.1 %
1.8 %
2.1 %
2.6 %
Pn/f'cobd
Mn/f'cobd2
0
0.5
1
1.5
2
2.5
0
0.1
0.2
0.3
0.4

(a)

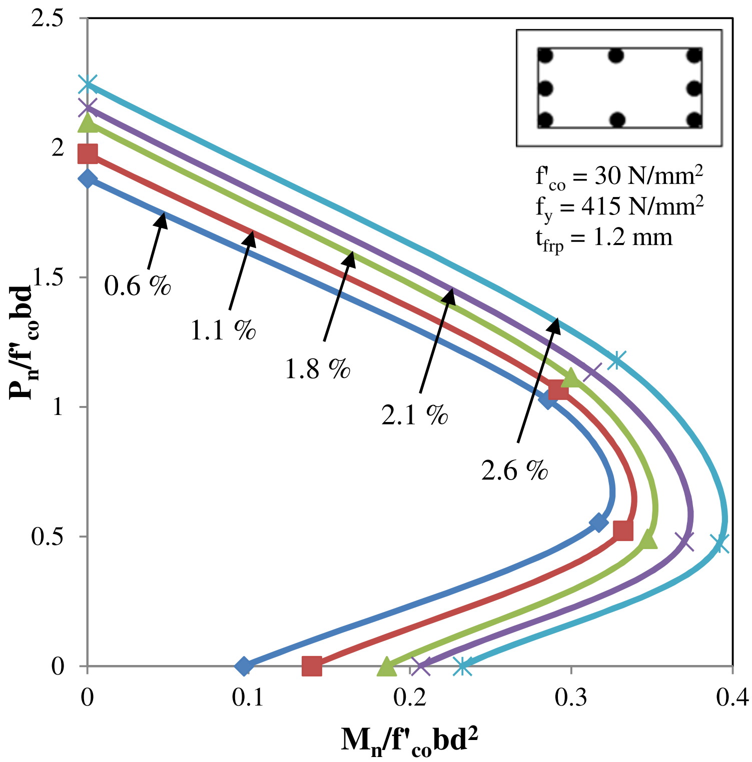
f'co = 30 N/mm2
fy = 415 N/mm2
tfrp = 1.2 mm
0.6 %
1.1 %
1.8 %
2.1 %
2.6 %
Pn/f'cobd
Mn/f'cobd2
0
0.5
1
1.5
2
2.5
0
0.1
0.2
0.3
0.4

(b)

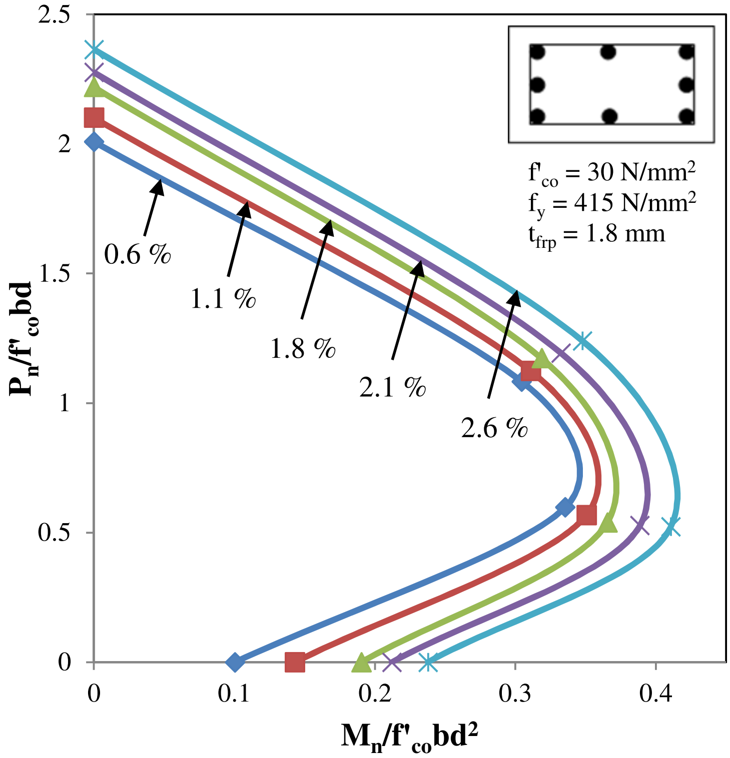

(c)

Fig. 7. P_n - M_n interaction diagrams for f'_{co} 30 N/mm^2 and f_y 415 N/mm^2 (a) t_{frp} 0.6 mm, (b) t_{frp} 1.2 mm and (c) t_{frp} 1.8 mm

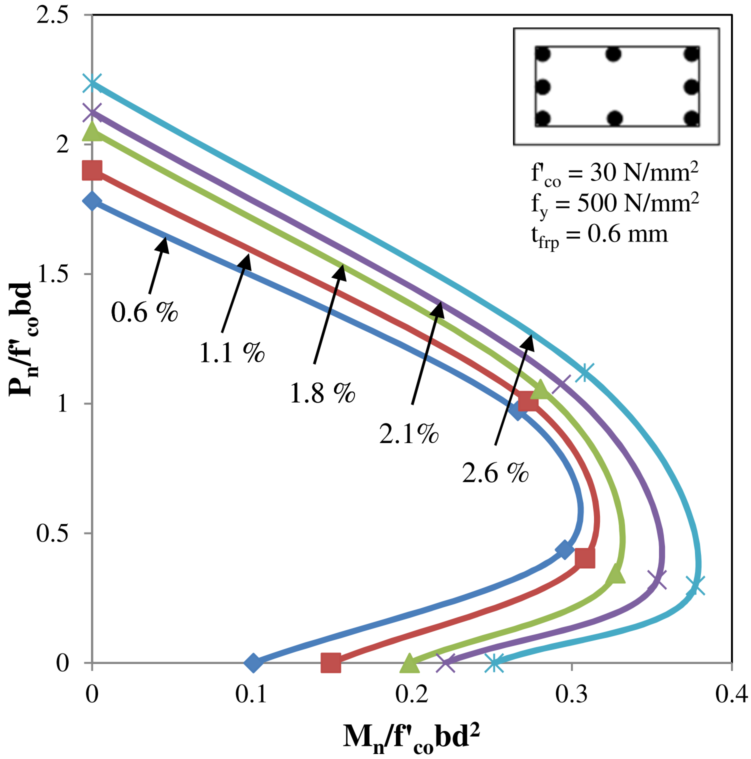

(a)

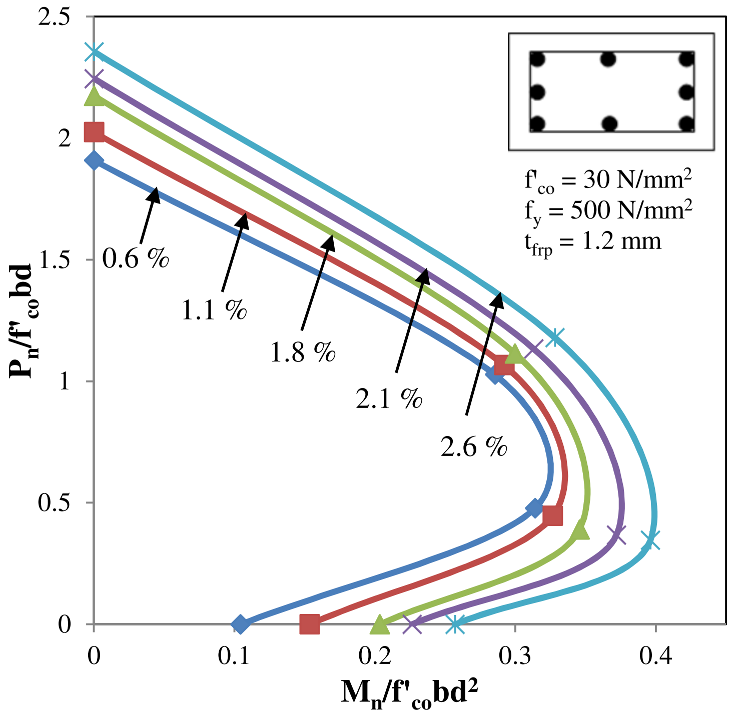

(b)

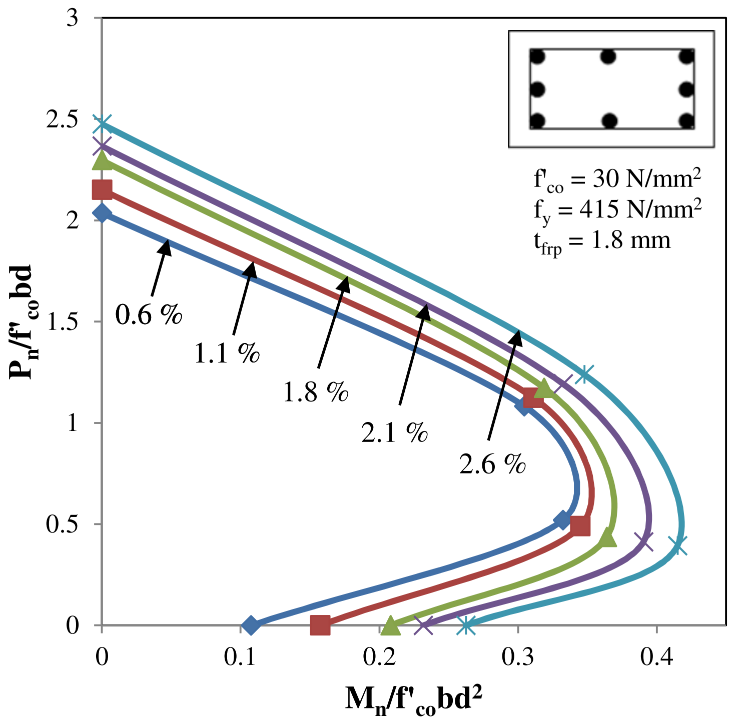

(c)

Fig. 8. P_n - M_n interaction diagrams for f'_{co} 30 N/mm^2 and f_y 500 N/mm^2 (a) t_{frp} 0.6 mm, (b) t_{frp} 1.2 mm and (c) t_{frp} 1.8 mm

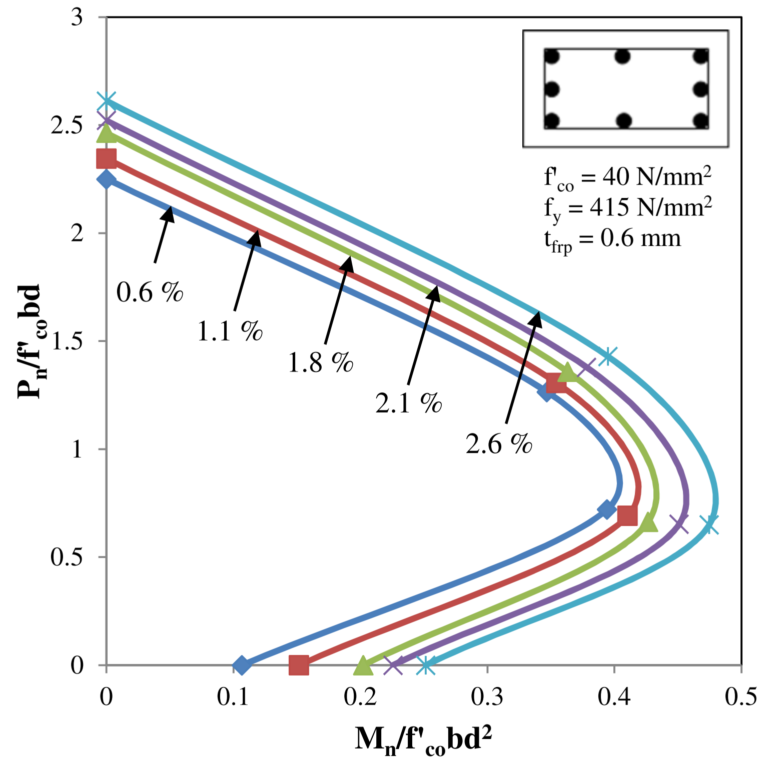

f'co = 40 N/mm2
fy = 415 N/mm2
tfrp = 0.6 mm
0.6 %
1.1 %
1.8 %
2.1 %
2.6 %
Pn/f'cobd
Mn/f'cobd2
0
0.1
0.2
0.3
0.4
0.5
0
0.5
1
1.5
2
2.5
3

(a)

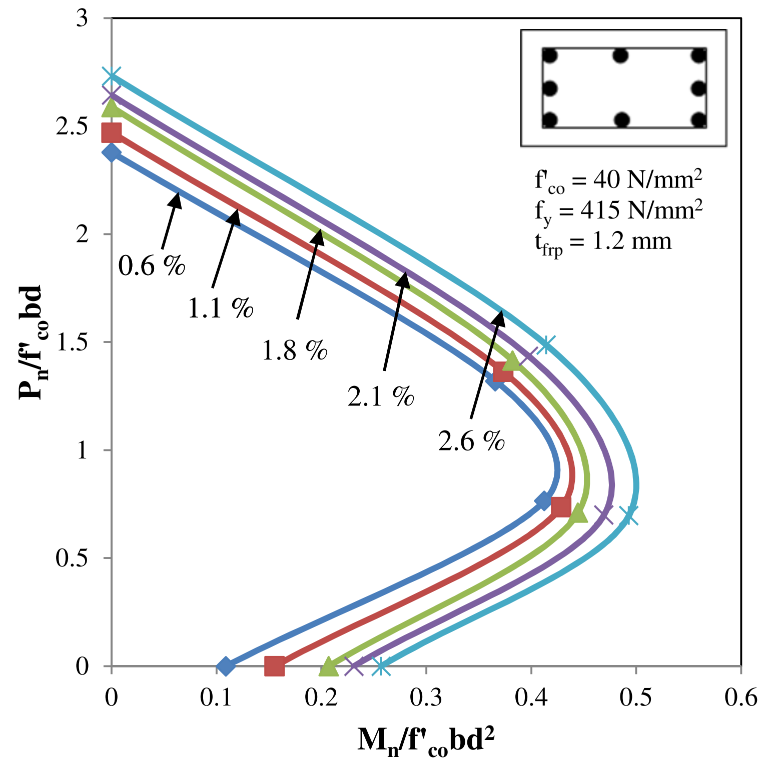

f'co = 40 N/mm2
fy = 415 N/mm2
tfrp = 1.2 mm
0.6 %
1.1 %
1.8 %
2.1 %
2.6 %
Pn/f'cobd
Mn/f'cobd2
0
0.1
0.2
0.3
0.4
0.5
0.6
0
0.5
1
1.5
2
2.5
3

(b)

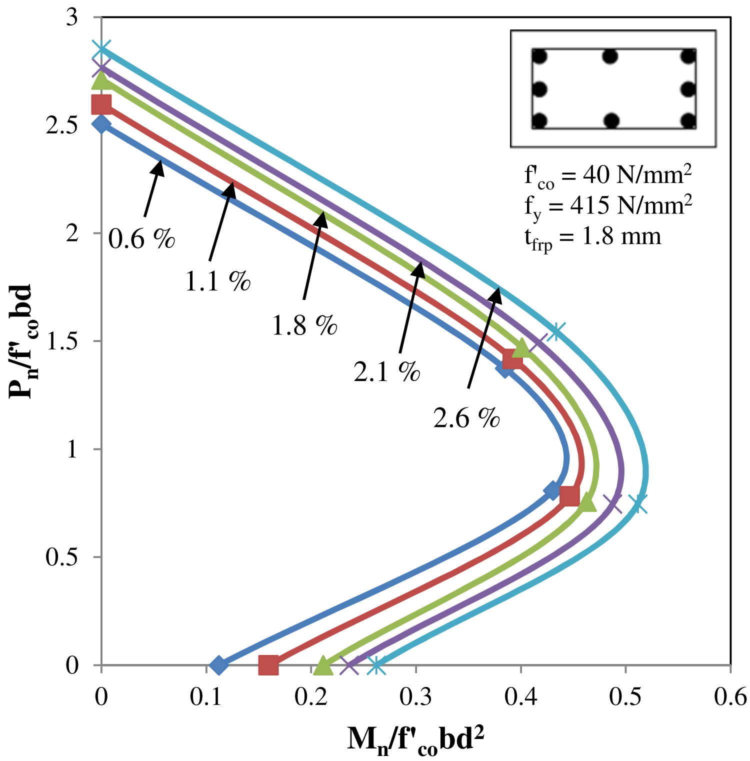

(c)

Fig. 9. P_n - M_n interaction diagrams for f'_{co} 40 N/mm^2 and f_y 415 N/mm^2 (a) t_{frp} 0.6 mm, (b) t_{frp} 1.2 mm and (c) t_{frp} 1.8 mm

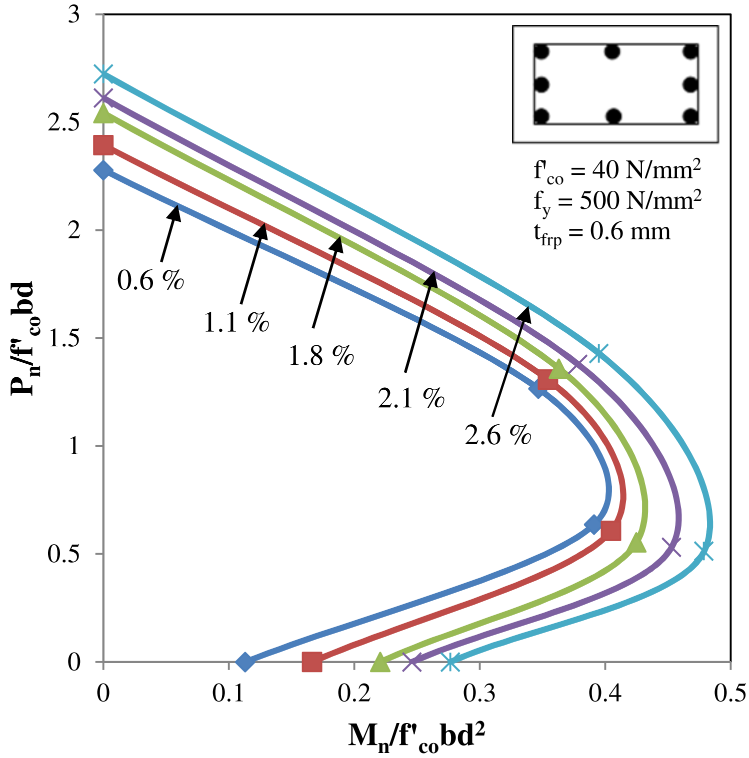

(a)

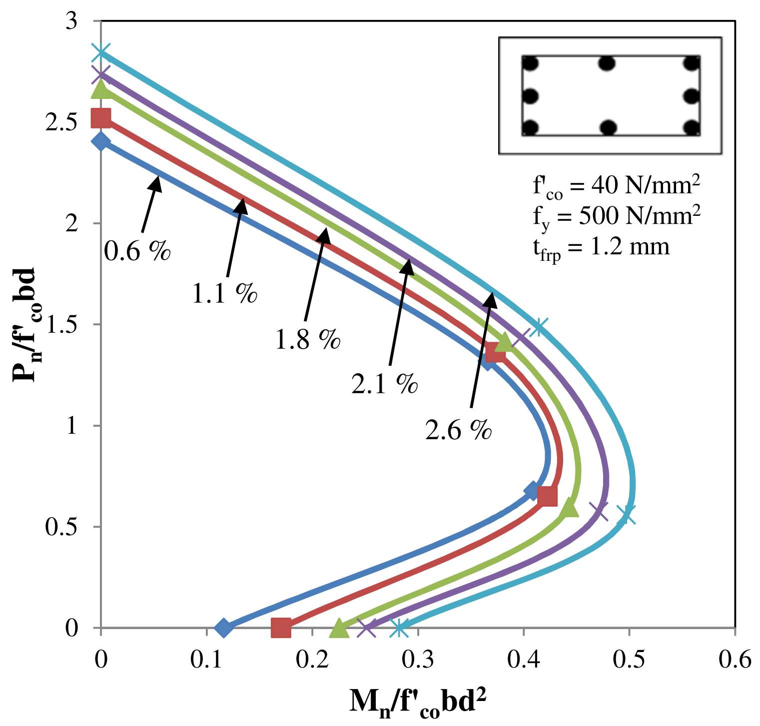

(b)

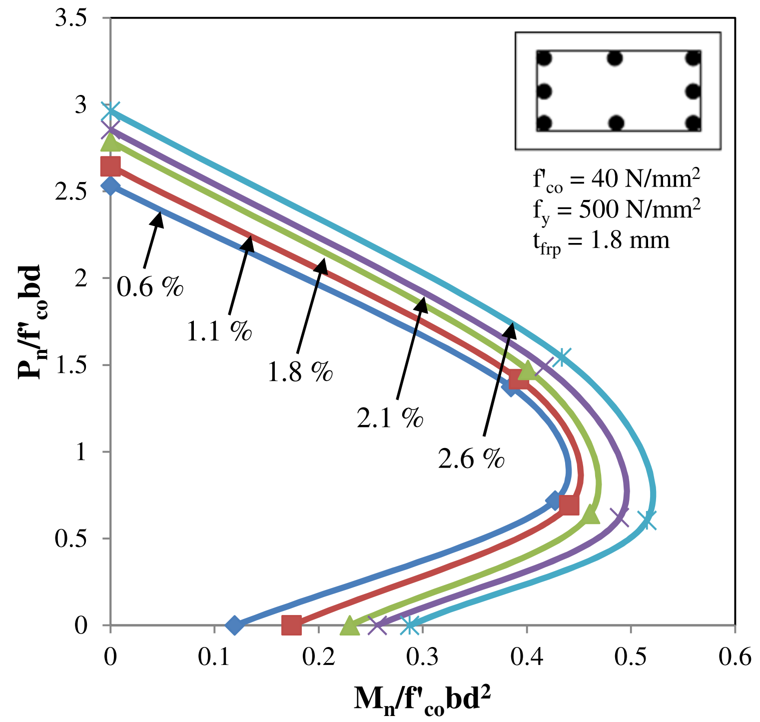

(c)

Fig. 10. P_n - M_n interaction diagrams for f'_{co} 40 N/mm^2 and f_y 500 N/mm^2 (a) t_{frp} 0.6 mm, (b) t_{frp} 1.2 mm and (c) t_{frp} 1.8 mm

7. Analysis Problem

Calculate the moment carrying capacity of a RC rectangular column strengthened with one layer of CFRP composite without shape modification subjected to uni axial bending with following data. Size of column – 200 mm × 500 mm, f'_{co} = 25 N/mm^2, f_y = 415 N/mm^2, Axial load - 1300 kN, Reinforcement Details – 4 no's of 20 mm dia. steel bars on two longer sides.

Assuming cover of 40 mm, Effective depth d= 160 mm

Percentage of steel reinforcement, $\rho_s = 2.51\%$

Thickness of FRP for one layer = 0.6 mm

For $f'_{co} = 20$ N/mm^2, $P_n / f'_{co}\, bd = 0.812$

From Fig. 5(a), $M_n / f'_{co}\, bd^2 = 0.22$

Therefore, $M_n = 56.3$ kN m

Similarly, For $f'_{co} = 30$ N/mm^2, $P_n / f'_{co}\, bd = 0.54$

From Fig. 7(a), $M_n / f'_{co}\, bd^2 = 0.37$

Therefore, $M_n = 142$ kN m

From linear interpolation, For $f'_{co} = 25$ N/mm^2, $M_n = 100$ kN m

For the same column details moment carrying capacity is obtained as 110 kN m from semi-empirical equations. So, the load carrying capacity of columns for different values other than the specified values of parameters given in interaction diagrams can be obtained by linear interpolation.

8. Summary and Conclusions

Semi-empirical solutions proposed by ACI 440.2R-08 for columns with an aspect ratio less than 2.0 are modified to predict the lateral capacities of RC rectangular columns having aspect ratio greater than 2.0 strengthened using FRP composites and without any shape modification and subjected to combined axial and lateral loading. 3D finite element models for RC rectangular columns strengthened with FRP composites are generated using FEA software ABAQUS. The failure pattern and load/deflection curve obtained from FEA is compared and validated with the corresponding tested specimens. P_n - M_n interaction diagrams are generated from the FE models and semi-empirical solutions and compared. P_n - M_n interaction diagrams are developed using the proposed semi-empirical solutions by varying parameters such as unconfined compressive strength of concrete (f'_{co}) and yield strength of steel (f_y), percentage of steel reinforcement (ρ_s) and thickness of FRP composite (t_{frp}).

The following major conclusions are drawn from this study.

1. The proposed semi-empirical solutions shall be used to predict the lateral load carrying capacity of FRP strengthened RC rectangular columns having aspect ratio greater than 2.0 and without shape modification of cross section.
2. Finite element models are validated well with the semi-empirical solutions and can be used for developing P_n - M_n interaction diagrams.
3. P_n - M_n interaction diagrams obtained from this study shall be used for the design of strengthening of RC rectangular columns with large aspect ratio and without shape modification.

9. Suggestions for Future Work

Prototype FRP strengthened RC rectangular columns having different aspect ratios greater than 2.0 shall be tested under combined axial and lateral loading and the developed P_n - M_n interaction diagrams can be further validated

Acknowledgements

The authors would like to express their appreciation to the Structural Engineering Laboratory, Civil Engineering Department, IIT Madras for the financial support of this research #CE13D055.

REFERENCES

1. ACI 440.2R-08. Guide for the Design and Construction of Externally Bonded FRP Systems for Strengthening Concrete Structures. Reported by ACI Committee 440.
2. Alsayed SH, Almusallam TH, Ibrahim SM, Al-Hazmi NM, Al-Salloum YA and Abbas H. Experimental and numerical investigation for compression response of CFRP strengthened shape modified wall-like RC columns. Constr build mater 2014;63:72-80.
3. Chaallal O, Hassan M and Shahawy M. Confinement model for axially loaded short rectangular columns strengthened with fiber reinforced polymer wrapping. ACI Struct. J 2003;100(2):215–221.
4. Chen L and Togay O. Corner strengthening of square and rectangular concrete-filled FRP tubes. Eng Struct 2016;117:486-495.
5. Lam L and Teng JG. Design oriented stress-strain model for FRP-confined concrete. Constr build mater 2003;17:471-489.
6. Parvin A and Jamwal AS. Performance of externally FRP reinforced columns for changes in angle thickness of the wrap and concrete strength. Compos Struct 2006;73:451-457.
7. Pedro F, Carlos C and Raquel P. Design model for square columns under compression confined with CFRP. Compos Struct: Part B 2014;57:187-198.
8. Prota A, Manfredi G and Cosenza E. Ultimate behavior of axially loaded RC wall-like columns confined with GFRP. Compos Struct: Part B 2006;37:670-678.
9. Mirmiran A and Shahawy M. Behavior of concrete columns confined by fiber composites. J Struct Eng 1997;123(5):583-590.

10. Mohammad RI, Mohammed HA and Mahmoud A. Strengthening RC columns using carbon fiber reinforced epoxy composites modifies with carbon nanotubes. International J of Civil, Environmental, structural, Construction and Architectural Engineering 2015;9(1):19-22.

11. Seible F, Priestley MJN, Hegemier GA and Donato I. Seismic retrofit of RC column with continuous carbon fibre jackets. J Compos Constr 1997;1(2):52-62.

12. Sreelatha Vuggumudi and P Alagusundaramoorthy. FRP strengthened RC Rectangular Columns under Combined Axial and Lateral Loading: Analytical Study. Structures 2018;14: 88-94.

13. Tan KH. Strength enhancement of rectangular reinforced concrete columns using fiber-reinforced polymer." J Compos Constr 2002; 6(3):175-183.

14. Tanwongsval S, Maalej M and Paramasivam P. Strengthening of RC wall-like columns with FRP under sustained loading. Materials and structures 2003;36:282-290.

15. Teng JG and Lam L. Compressive behavior of carbon fiber reinforced Polymer-confined concrete in elliptical columns. J Struct Eng 2002;128(12):1535-1543.

16. Teng JG and Lam L. Behavior and modeling of fibre reinforced polymer-confined concrete. J Struct Eng 2004;130(11):1713-1723.

17. Wang YC and Hsu K. Design of FRP-wrapped reinforced concrete columns for enhancing axial load carrying capacity. Compos Struct 2008;82:132-139.

Figure Captions

Fig. 1. Representative Interaction Diagram

Fig. 2. Failure Pattern of Column RCC6 (a) Test (b) FEA

Fig. 3. Lateral Load/Lateral Deflection Curves of Column RCC6

Fig. 4. Comparison of P_n - M_n interaction diagram

Fig. 5. P_n - M_n interaction diagrams for f'_{co} 20 N/mm^2 and f_y 415 N/mm^2 (a) t_{frp} 0.6 mm, (b) t_{frp} 1.2 mm and (c) t_{frp} 1.8 mm

Fig. 6. P_n - M_n interaction diagrams for f'_{co} 20 N/mm^2 and f_y 500 N/mm^2 (a) t_{frp} 0.6 mm, (b) t_{frp} 1.2 mm and (c) t_{frp} 1.8 mm

Fig. 7. P_n - M_n interaction diagrams for f'_{co} 30 N/mm^2 and f_y 415 N/mm^2 (a) t_{frp} 0.6 mm, (b) t_{frp} 1.2 mm and (c) t_{frp} 1.8 mm

Fig. 8. P_n - M_n interaction diagrams for f'_{co} 30 N/mm^2 and f_y 500 N/mm^2 (a) t_{frp} 0.6 mm, (b) t_{frp} 1.2 mm and (c) t_{frp} 1.8 mm

Fig. 9. P_n - M_n interaction diagrams for f'_{co} 40 N/mm^2 and f_y 415 N/mm^2 (a) t_{frp} 0.6 mm, (b) t_{frp} 1.2 mm and (c) t_{frp} 1.8 mm

Fig. 10. P_n - M_n interaction diagrams for f'_{co} 40 N/mm^2 and f_y 500 N/mm^2 (a) t_{frp} 0.6 mm, (b) t_{frp} 1.2 mm and (c) t_{frp} 1.8 mm